Journal of Power Sources 269 (2014) 7–14

Contents lists available at ScienceDirect

Journal of Power Sources

journal homepage: www.elsevier.com/locate/jpowsour

State of health and charge measurements in lithium-ion batteries using mechanical stress

John Cannarella, Craig B. Arnold*

Department of Mechanical and Aerospace Engineering, Princeton University, Princeton, NJ 08544, USA

HIGHLIGHTS

- Mechanical stress can be used to monitor SOH and SOC.
- Stress is linearly related to state of health.
- The linear stress-SOH relationship holds over range of cycling conditions.
- Data suggests SEI growth is responsible for the observed stress-SOH relationship.
- A phenomenological model can explain linear stress-SOH relationship.

ARTICLE INFO

Article history:
Received 11 February 2014
Received in revised form
28 May 2014
Accepted 1 July 2014
Available online 9 July 2014

Keywords:
Mechanical stress
Lithium-ion battery
State of charge (SOC)
State of health (SOH)
Battery management system
Solid electrolyte interface (SEI)

ABSTRACT

Despite the fundamental importance of state of health (SOH) and state of charge (SOC) measurement to lithium-ion battery systems, the determination of these parameters is challenging and remains an area of active research. Here we propose a novel method of SOH/SOC determination using mechanical measurements. We present the results of long term aging studies in which we observe stack stress to be linearly related to cell SOH for cells aged with different cycling parameters. The observed increases in stack stress are attributed to irreversible volumetric expansion of the electrodes. We discuss the use of stress measurements for SOC determination, which offers the advantage of being more sensitive to SOC than voltage as well as the ability to measure SOC in the presence of self discharge. Finally we present a simple model to explain the linear nature of the observed stress-SOH relationship. The inherent simplicity of the mechanical measurements and their relationships to SOH and SOC presented in this paper offer potential utility for the improvement of existing battery management systems.

1. Introduction

The determination of state of health (SOH) and state of charge (SOC) is critical for efficient operation and management of lithium-ion battery systems. This is especially important for applications such as electric vehicles where unexpected depletion of the battery pack can have dire consequences. To this end there has been a large body of work focusing on developing methods of estimating SOH and SOC in lithium-ion batteries during operation in real time [1,2,3,4,5,6]. There is some ambiguity over the definitions of SOH and SOC, so these terms will be defined here as they are used in the remainder of this paper. The SOH is here defined as the available capacity of a fully charged battery as a percentage of its original full capacity. The SOC is here defined as the percentage of remaining available capacity. For example, a 1 Ah cell at 90% SOH and 50% SOC will have an available remaining capacity of 0.45 Ah.

The most accurate method of SOH/SOC measurement is through a controlled discharge test, but such a test cannot be implemented as a real time measurement technique and is best suited for laboratory settings. To this end many techniques have been pursued in the literature for real time state estimation in batteries, without having to rely on a controlled discharge. These techniques estimate SOH/SOC based on measurable parameters (e.g. voltage, current, temperature) through the use of an underlying model. These models include both physical models, empirical models, or some combination of the two [3]. The models range from complex systems of differential equations to simpler equivalent circuit based models, but generally require complicated calculations to relate measurable parameters to SOH and SOC [3]. The accuracy of these methods depend on the accuracy of the underlying models and is

* Corresponding author.
E-mail address: cbarnold@princeton.edu (C.B. Arnold).
URL: http://www.princeton.edu/~spikelab

http://dx.doi.org/10.1016/j.jpowsour.2014.07.003
0378-7753/

further complicated by changes in the battery system that arise with aging.

Here we introduce the possibility of using easily measurable mechanical parameters, stress and strain, to compliment existing battery management methods or even act as a standalone method for determining SOH and SOC. The mechanical stress that will be referred to in this paper is the uniaxial stress that arises within the battery cell as a result of electrode expansion against a constraint in the direction normal to the plane of the electrodes. This stress is different from stresses arising within the plane of the electrode and from stresses arising within individual electrode particles, which have been the subjects of many studies [7,8,9,10,11]. Unlike stress within individual particles or within the electrode plane, stack level stress can be measured easily for a pouch cell by placing a load cell in series with the pouch cell in a rigid constraint as described in previous work [12]. While this study focuses on measurements of mechanical stress, an analogous study could be conducted using strain measurements of cells during aging, as the stress measured in this study can be considered a measurement of cell strain.

The study in Ref. [12] shows that stack stress is a dynamic quantity during cell operation, fluctuating with SOC as a result of electrode charging strains and gradually accumulating over the life of the cell. This work more closely investigates the relationship between SOH, SOC, and the stack level mechanical stress that is measured during battery operation, with the intention of using the measured stress as an SOH/SOC estimation technique. While only a single lithium-ion chemistry is considered here, the described stress-based SOH/SOC methods should be generally applicable to any system that exhibits volumetric changes that are related to SOH and SOC. The simplicity of the mechanical measurements and straightforward nature of the stress-SOH and stress-SOC relationships presented in this paper offer distinct advantages to the more complex current state of the art.

2. Experimental methods

The commercial LCO/C pouch cells and the apparatus used for mechanically constraining the cells and monitoring stack stress are described in Ref. [12]. Note that the cells used in this work are mechanically stiffer than those in Ref. [12] owing to the use of a thinner separator. This difference in mechanical properties causes slight quantitative changes to the mechanical behavior of the cells during cycling, but does affect the qualitative behavior. Commercial cells are used to ensure the relevancy of this work to practical cells fabricated by industry, which are generally of higher manufacturing quality [13]. All cells in this study are discharged to the 2.7 V lower voltage limit and then subsequently constrained with an initial stack pressure of 0.05 MPa. The 0.05 MPa stack pressure has previously been shown to be near optimal for maximizing the cycle life of the cells used in this study [12]. Lower stack pressures also have the advantage of reducing the effects of stress relaxation, which can introduce transient decreases in stack stress at early times, obscuring changes in stress resulting from volumetric expansion of the cell electrodes.

The constrained cells are then cycled with different cycling parameters to flesh out the effects of cycling conditions on the mechanical stress evolution during cycling. This study considers cells cycled using a 4.2 V CCCV scheme with currents of 0.25 C, 0.5 C, 1 C, 1.5 C and 2 C. Cells aged by holding at 4.2 V are also considered. The 0.5 C CCCV cells and 4.2 V hold cells are aged both at ambient room temperature (21–23°C) and at an elevated temperature of 55 °C. Elevated temperatures between 45 °C and 65 °C have been used in previous studies to accelerate aging, especially through SEI growth mechanisms [3,14,15,16]. All other cells are cycled only in ambient room temperature. Three cells are cycled in each condition to ensure repeatability of results. All cells are periodically cycled at a C/10 rate to determine capacity, regardless of the parameters used for cycling the cells. The use of a uniform discharge rate across all cells allows for more accurate comparison of capacity values. The slow discharge also allows for differential voltage spectroscopy (dV/dQ) analysis of the cells, which has been used provide non-destructive analysis of aging mechanisms in numerous studies [14,17,15,18].

3. Results and discussion

3.1. SOH and mechanical stress

A plot of the stress evolution of a cell aged using a C/2 CCCV scheme at 55 °C is shown in Fig. 1a. This figure shows two curves corresponding to the cell stack stress at the fully charged state ("Peak stress 4.2 V") and at the discharged state ("2.7 V cutoff"). The region bounded by these two curves contains stress levels at intermediate SOCs that are traversed by the cell during cycling. Both curves slope upward, representing an irreversible accumulation of stack stress with cycling. The upward slope is more pronounced in the charged state due to the cell's stress-dependent stiffness discussed previously [12]. The trend of increasing stack stress with cycling shown in Fig. 1a is generally representative of the stress evolution behavior of all cells aged by cycling under low stack pressures observed in this and previous work [12].

We attribute this irreversible increase in stack stress to permanent volumetric expansion of the cell electrodes, in particular the graphite anode, which we observe to be thicker after cycling [12]. Similar observations of irreversible electrode expansion and stress generation, particularly in graphite electrodes, have been reported previously in the literature [19,20,7,8,9,12,21,22,23,24,25,26]. To verify that electrode expansion is indeed the responsible for the observed stress changes, we conducted the following control experiment to rule out the possibility of a contribution from a hydrostatic pressure source such as gas evolution. We cut a slit in the pouch of a cell such that gas is able to escape and no gas pressure can build up, and then cycled this cell under Argon atmosphere. The slit pouch cell exhibits the same mechanical behavior as the un-slit pouch cells as shown in Fig. 2, confirming that electrode expansion is responsible for the measured stress increases. Furthermore, none of the cells in this study exhibited noticeable bloating, which would be expected for any cells exhibiting significant gas evolution.

The irreversible increases in stack stress are related to capacity fade such that a linear relationship emerges when stack stress is plotted against SOH as seen in Fig. 1c. The stress-SOH relationship shown in Fig. 1c is constructed by plotting the peak stress from Fig. 1a against the corresponding C/10 discharge capacity from Fig. 1b. Each data point on the stress-SOH curve in Fig. 1 represents the C/10 discharge capacity measured between sets of 50 C/2 CCCV cycles. In the case of the cell presented in Fig. 1, there is little difference between the C/2 and C/10 discharge capacities. This distinction becomes more important for cells exhibiting larger resistive losses at higher rates. Both the peak stress curve and in Fig. 1a and the SOH curve in Fig. 1b show $t^{1/2}$ behavior (see Fig. 1d), which is indicative of capacity fade through a diffusive mechanism such as SEI growth [3,14,15].

Representative stress-SOH curves exhibiting the same linear relationship as seen in Fig. 1c are shown in Fig. 3 for cells aged by CCCV cycling under the following conditions: C/2 at 22 °C, C/2 at 55 °C, and C/4 at 22 °C. Fig. 3 differs from Fig. 1c in that the increase in peak stress is plotted instead of the actual peak stress. This stress increase in Fig. 3 is calculated by subtracting the initial peak stress at cycle 0 from the subsequent peak stress values such that all

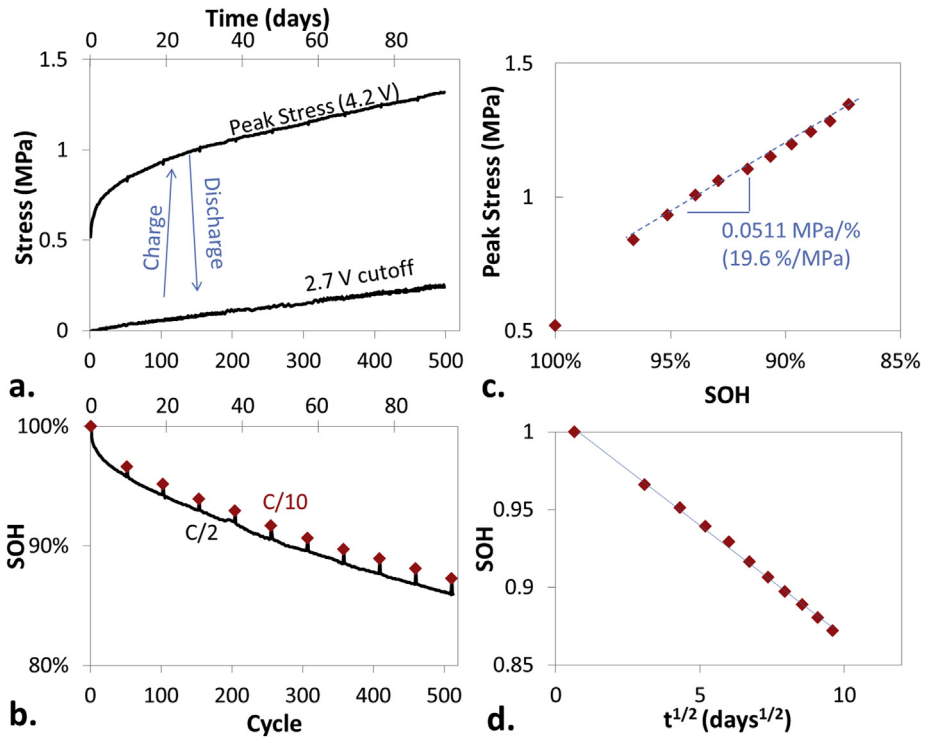

Fig. 1. Stack stress (a) and capacity (b) profiles used to construct a plot of stress vs. capacity (c) typical for a cell aged by cycling. The $t^{1/2}$ dependence of the cell's capacity fade is shown in (d). This specific cell is aged using a C/2 4.2 V CCCV scheme at 55°C with periodic C/10 cycles for capacity measurement.

curves start from 0 on the *x* axis. Note that the capacity measurements used to determine SOH in Fig. 3 are all made at a rate of C/10. The cells aged by cycling at rates above C/2 do not show the same linear relationship as cells aged at rates of C/2 and under, and are not shown in the figure. Cells cycled above C/2 showed higher rates of capacity fade and large increases in impedance, suggesting the onset of additional aging phenomena at higher charging rates. At rates of C/2 and below, the slope of the linear stress-SOH relationship appears to be independent of cycling rate.

In comparing cells cycled at room temperature and elevated temperature, Fig. 3 shows that temperature initially has little effect on the slope of the stress-SOH curve. However, the linear relationship between SOH and stress breaks down for the cells cycled at 22 °C after about 200 cycles, after which the SOH begins to decrease without a corresponding increase in peak stress. This change in stress-SOH behavior is indicative of a change in capacity fade mechanism to a mechanism that is not coupled to volumetric expansion. This assertion of a change in capacity fade mechanism is supported by differential voltage spectroscopy measurements of the cells during the periodic C/10 discharges, which show a change

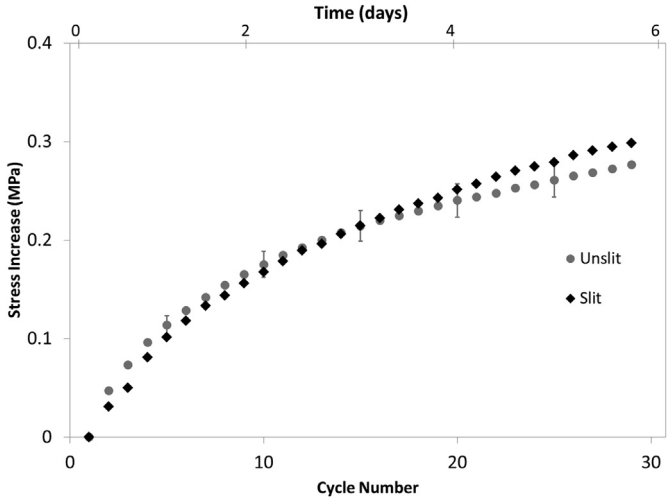

Fig. 2. Plot of stack stress increase verses cycle for a slit pouch cell and three unslit pouch cells cycled under a C/2 CCCV scheme at room temperature. The data for the three unslit pouch cells are represented as an average with periodic error bars showing ± one standard deviation.

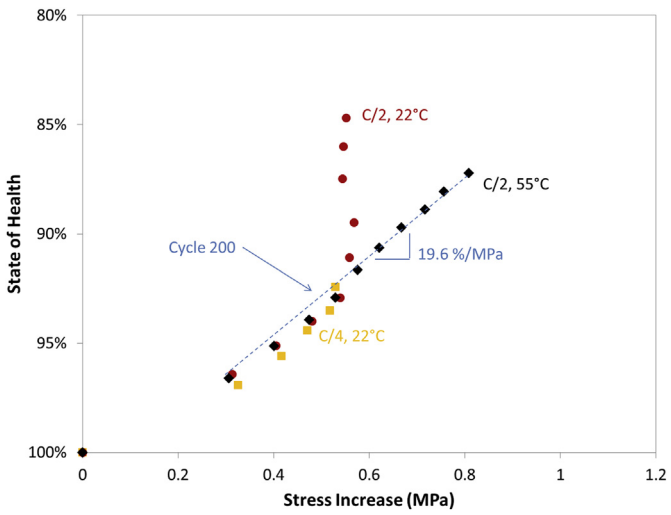

Fig. 3. SOH as a function of stress increase for cells aged by CCCV cycling. SOH is determined by a C/10 capacity measurement between sets of 50 CCCV cycles.

in behavior starting near cycle 200 in the 22 °C cells compared to the 55 °C cells.

Representative dV/dq curves for the 55 °C cells and the 22 °C cells are shown in Fig. 4a and b, respectively. The feature marked "LCO" is characteristic of the LCO cathode discharge voltage curve and the feature marked "C" is characteristic of the graphite anode discharge voltage curve, as determined from half cell measurements of individual electrodes harvested from pristine cells. In the set of dV/dq curves for the 55 °C cells in Fig. 4a, the cathode feature occurs at the same discharge capacity over the life of the cell, as denoted by the vertical dashed line. The anode feature shifts to lower discharge capacities, exhibiting the same $t^{1/2}$ dependence as the SOH curve from Fig. 1b. This behavior is characteristic of capacity fade through a lithium loss mechanism, with the $t^{1/2}$ dependence suggesting SEI growth [14,17,15].

The dV/dq curves for the 22 °C cells in Fig. 4b show similar behavior to the 55 °C cells up until around cycle 200, after which the LCO feature begins shifting to lower discharge capacities as indicated by the change in slope of the dashed LCO line. Simultaneously, the graphite feature begins to deviate from the expected $t^{1/2}$ behavior which was exhibited by the 55 °C cells. The change in behavior around cycle 200 indicates the onset of an alternative capacity fade mechanism, which can be correlated to the change in the stress-SOH relationship near the same number of cycles for the 22 °C C/2 cell in Fig. 3. The simultaneous shifting of both electrodes is characteristic of a mechanism that makes both electrodes appear to have lost capacity, such as loss of contact or electrolyte [19]. Such a mechanism would not be expected to produce an increase in stack stress, consistent with Fig. 3.

Aging cells by holding at 4.2 V provides further insight into the physical basis for the relationship between stress and SOH. Stress and SOH data for a cell aged by holding at 4.2 V at room temperature is presented in Fig. 5. This cell is cycled at a C/10 rate every 20 days to determine capacity, which is responsible for the periodic drops in stress in the stress–time curve in Fig. 5a. As is the case with the cells aged by repeated cycling, the SOH curve in Fig. 5b follows a $t^{1/2}$ dependence as shown in Fig. 5d, suggestive of an SEI growth mechanism. The stack stress of the cells aged by constant voltage holding increases with each cycle, similar to the cells aged by cycling. At later times, the stress can also be seen increasing between C/10 cycles, indicating that the cell is expanding with time during the twenty day voltage holds in the absence of cycling. Stress increases in the absence of cycling rule out a purely mechanical mechanism such as reconfiguration of particles within the composite electrode [23]. The aggravation of stress accumulation with both cycling and time is similar to the behavior of capacity fade that proceeds through an SEI growth mechanism [15]. Plotting stress against SOH in Fig. 5c reveals a stress-SOH relationship with similar slope to those seen in Fig. 3, suggesting the same aging mechanism behind the cells aged at 4.2 V and the cells aged by cycling.

Construction of the stress-SOH curves for the cells aged by holding at 4.2 V is complicated by stress relaxation, which causes a noticeable decline in stack stress between C/10 cycles during the first 200 days in Fig. 5a. Consequently, there are a range of stress values during each voltage hold step that can be used to construct stress-SOH curves. For example, the stress immediately following or preceding a C/10 cycle can be used as the stress measurement for the SOH measured on that cycle. These points are marked as orange and red (in the web version) in Fig. 5, respectively. This results in the two stress-SOH curves shown in Fig. 5c. The stress measurements immediately preceding the C/10 cycle have the advantage of being made after the stress has relaxed for 20 days, which reduces the effects of stress relaxation on the corresponding stress-SOH curve. Consequently, the orange curve occurs at higher stresses than the red curve, especially at early times where the rate of stress relaxation is highest. Eventually the slopes of the two stress-SOH curves begin to converge as the rate of stress relaxation diminishes at later times, approaching the slope of the stress-SOH curves of the cycled cells in Fig. 3. The similarity in slope of the stress-SOH curves suggests the same mechanism of capacity fading and of stress-SOH coupling is occurring in both sets of cells.

The stress relaxation exhibited by the cells aged by constant voltage holding is not noticeable in cells aged by cycling in Fig. 1a.

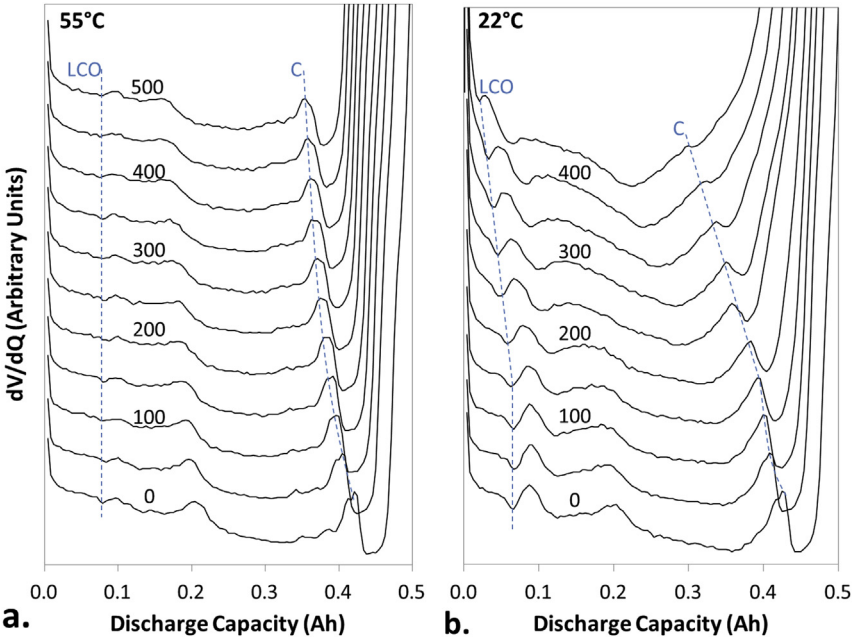

Fig. 4. Differential voltage spectra for cells aged using a C/2 CCCV scheme at a) room temperature and at b) elevated temperature. Each trace is taken during a C/10 discharge between sets of 50 CCCV cycles.

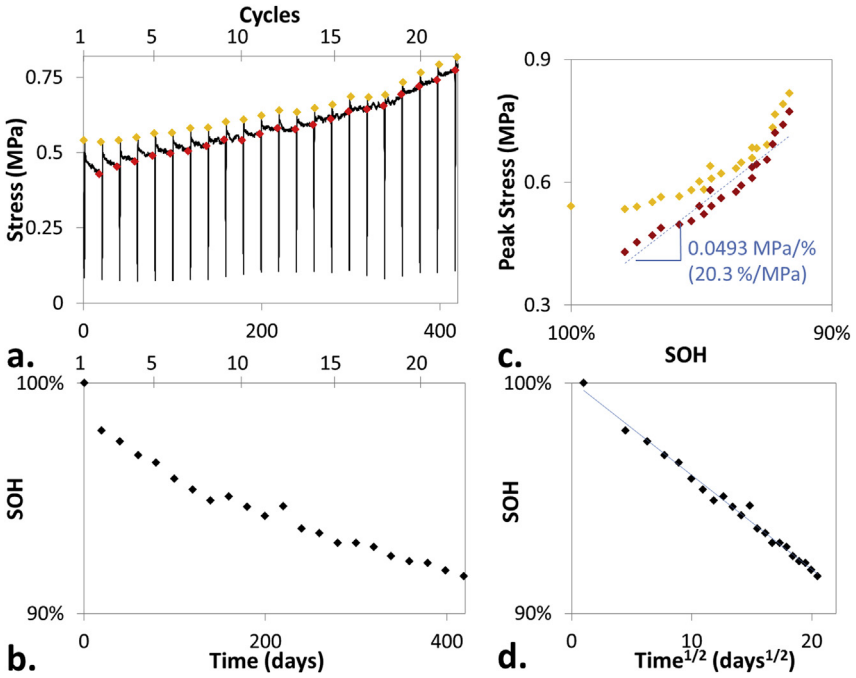

Fig. 5. Stack stress (a) and capacity (b) profiles used to construct a plot of stress vs. capacity (c) typical for a cell aged by holding at a constant voltage. The $t^{1/2}$ dependence of the cell's capacity fade is shown in (d). This specific cell is aged by holding at 4.2 V with periodic C/10 cycles for capacity measurement.

The absence of noticeable stress relaxation in Fig. 1a is because the high rate of stress accumulation due to irreversible expansion from cycling overshadows the simultaneously occurring stress relaxation. Although the presence of stress relaxation is not obvious in the cells aged by cycling, stress relaxation still occurs in these cells, as stress relaxation is a purely mechanical phenomenon. This stress relaxation is primarily due to the viscoelastic response of the polymeric components of the cell, in particular, the separator [27,28]. The opposite behavior is exhibited by cells aged by constant voltage holding, where the high rate of stress relaxation overshadows the simultaneously occurring irreversible expansion with aging in between cycles during the first 200 days in Fig. 5a. The irreversible expansion is obscured in this case because the time-rate of irreversible expansion is much slower in the absence of cycling. At later times the rate of stress relaxation diminishes and is dominated by stress accumulation from irreversible expansion. The necessity to account for stress relaxation is a disadvantage inherent to using mechanical stress as a proxy for cell expansion.

For the cells aged by holding at 4.2 V, aging at elevated temperature results in a significant acceleration of both capacity fade

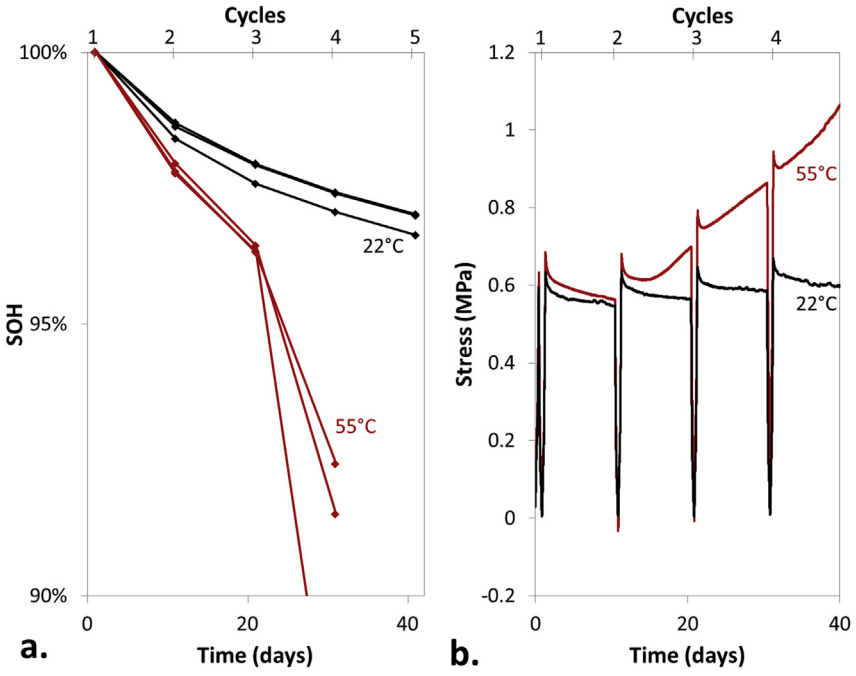

Fig. 6. Comparison of capacity (a) and stack stress (b) evolution for cells aged by holding at 4.2 V at room temperature and elevated temperature.

and stress increase as shown in Fig. 6. The acceleration of capacity fade with elevated temperature seen in Fig. 6a is a common observation in studies of temperature-dependant aging mechanisms such as SEI growth [3,14,15]. The simultaneous acceleration of stress accumulation seen in Fig. 6b corroborates the causal nature of the stress-SOH relationship, with lithium loss resulting in an increase in stack stress. The accelerated rate of irreversible stress increase in the 4.2 V cells aged at elevated temperature suggests a chemical mechanism for the observed irreversible stress increases, as chemical phenomena are expected to be accelerated with higher temperatures. The acceleration of stress increase with higher temperature rules out a purely mechanical mechanism such as reconfiguration of particles within the composite electrode [23], which is not expected to be accelerated with higher temperature. Also note that the elevated temperature cells also show a higher rate of stress relaxation, which is evidenced by the steeper downward slope of the stress curve for the 55°cell during the first 10 days in Fig. 6b. Accelerated stress relaxation at higher temperatures is expected, as battery separators exhibit weaker mechanical properties at higher temperatures [29,30,31]. In the elevated temperature cells, the rate of stress increase due to irreversible expansion exceeds the rate of stress relaxation between days 10 and 20, at which point the stress continuously increases. After 40 days, the elevated temperature cells all began to exhibit measurable rates of self discharge and testing was halted.

3.2. SOC and mechanical stress

Mechanical stress measurements can also be used to monitor the SOC of a constrained lithium-ion cell. The working principle of the stress-SOC relationship is the well known phenomenon of electrode expansion with lithium concentration [32,33,34,35,24]. By measuring changes in stack stress, which correspond to thickness changes of the electrodes, it is possible to determine SOC if a stress-SOC relationship for a given cell is known. Using stack stress measurements to determine SOC is advantageous because in many systems stress is more sensitive to SOC than conventionally used parameters such as voltage. This is especially true in two phase systems where the discharge curves are essentially flat with respect to SOC. Furthermore, we expect the stress-SOC relationship to be relatively independent of parameters such as current and temperature, which can significantly alter voltage measurements. The use of mechanical stress to determine SOC also offers the advantage of being able to measure self discharge, because stress/expansion is directly related to the lithium content in the electrodes. Conventional coulomb counting methods which measure charge passed through an external circuit cannot resolve internal discharge.

The stress-SOC relationship is dependent on the SOH of the cell as shown in Fig. 7. This dependence on SOH is a result of the irreversible thickness increase that occurs during cell aging, which results in a shift of all stress measurements to higher stresses as the electrodes irreversibly expand with decreasing SOH. Additionally, as the overall level of stress in the cell increases, the slopes of the stress-SOC curves change as seen in Fig. 7. This is a result of the non linear-elastic stress-strain behavior of the pouch cells, which exhibit higher stiffness at higher levels of stress as seen in previous work on mechanical properties of lithium-ion cells [36,12].

The stress-SOC relationship further varies with SOH due to the fact that the amount of lithium stored in each electrode decreases with decreasing SOH. Assuming lithium loss is the sole aging mechanism, the variation of electrode utilization with SOH can be easily seen by writing an expression for the lithium stored in the electrode as a function of SOC and SOH. For example, the lithium inventory stored in the anode q_a is

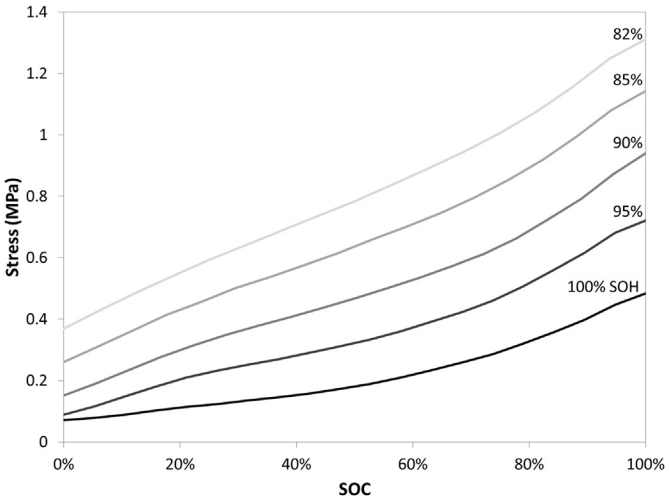

Fig. 7. Stress as a function of SOC for a cell at different states of health.

$$q_a = q_0(\mathrm{SOC})(\mathrm{SOH}), \tag{1}$$

where q_0 is the initial cell capacity. A similar expression can be written for the lithium inventory in the cathode by replacing the SOC term in Eq. (1) with (1-SOC). Eq. (1) shows that as SOH decreases, q_a for a specific SOC also decreases because less lithium is stored in the electrode at that specific SOC. For materials that expand when lithiated, this decrease in utilization results in a decrease in thickness at a given SOC, and consequentially a decrease in stack stress for a constrained cell.

3.3. Stress-SOH/SOC relationships for battery monitoring

In this section we will explain the observed linear stress-SOH relationship by considering how cell expansion evolves with SOH, and then relating cell expansion to stress. For simplicity, we limit this analysis to only considering the stress-SOH of a fully charged cell and we assume that all capacity fade is due to irreversible consumption of cycleable lithium, and not to degradation of individual electrodes. This assumption is valid for the cells considered in this study, and generally valid for a well-designed battery cell where the preferred failure mechanism is gradual SEI growth. We start by writing the thickness of the cell l_{cell} as a summation of thickness contributions from the anode l_a, cathode l_c, irreversible expansion l_i, and separator and other inactive components l_s.

$$l_{\mathrm{cell}} = l_a + l_c + l_i + l_s \tag{2}$$

Since we are interested in analyzing cell expansion, we will consider strain ε, which we define here as change in thickness Δl normalized by initial cell thickness $l_{\mathrm{cell},0}$:

$$\varepsilon_j = \frac{\Delta l_j}{l_{\mathrm{cell},0}} \tag{3}$$

We will assume that there is no thickness change in the inactive components such that $\varepsilon_s = 0$. This assumption could be relaxed in a more detailed model to account for stress and time dependant deformation of the separator. Because we are only considering the cell at 100% SOC, the cathode will always be depleted of cycleable lithium such that $\varepsilon_c = 0$, regardless of the cell's SOH. Consequently $\varepsilon_{\mathrm{cell}}$ contains contributions from only the anode and irreversible expansion and can be written as:

$$\varepsilon_{\text{cell}} = \varepsilon_i + \varepsilon_a \tag{4}$$

Both ε_i and ε_a are defined as 0 at 100% SOC and 100% SOH such that $\varepsilon_{\text{cell}} = 0$ initially. Consequently, as SOH decreases, ε_i is positive-valued and ε_a is negative-valued, as illustrated schematically in Fig. 8. Fig. 8 shows that ε_a is negative-valued because less lithium is available for storage in the anode as SOH decreases, which results in a decrease in anode thickness at 100% SOC. The irreversibly consumed lithium produces an expansion of greater magnitude than the anode contraction, resulting in a net expansion of the cell. Both ε_i and ε_a are functions of SOH, and we assume that their magnitudes are proportional to capacity fade (1−SOH) such that

$$\varepsilon_i = k_i(1 - \text{SOH}) \tag{5}$$

$$\varepsilon_a = -k_a(1 - \text{SOH}) \tag{6}$$

where k_i and k_a are positive-valued constants of proportionality.

The assumption of a linear relationship between ε_i and capacity fade in Eq. (5) can be justified for systems in which capacity fade causes an irreversible volumetric increase on the surface of the electrode particles, which is the case for a mechanism such as SEI growth. Here we assume degradation occurs uniformly within the electrode, but it should be noted that non-uniformities can be important to degradation [12,37]. If the volume of the electrode particles is assumed to be much larger than the volumetric expansion of the particles, the increase in thickness of the electrode particles is equivalent to the increase in volume divided by the surface area of the particle. For a composite electrode comprised of multiple particle layers, increases in composite electrode thickness scale linearly with increases in thickness of the constituent particles. Thus ε_i is expected to scale with (1−SOH) as written in Eq. (5). The proportionality constant k_i depends on the particle and cell geometry as well as the volumetric properties related to the irreversible expansion.

The assumption of a linear relationship between ε_a and capacity fade in Eq. (6) is valid for anode materials in which expansion is proportional to lithium concentration. This is because the irreversible consumption of lithium directly reduces the amount of lithium stored within the anode at 100% SOC, as seen in Fig. 8. Thus the proportionality constant k_a in Eq. (6) depends on particle and cell geometry as well as the expansion characteristics of the anode material. The requirement of linear expansion can be relaxed slightly to only require linear expansion in the range of lithium concentration that corresponds to the range of decreased SOH. For example, if an anode exhibits linear expansion over a range of lithiation corresponding to a 20% reduction in capacity, then we expect the linear relationship in Eq. (6) between 100% and 80% SOH. Using a graphite anode as an example, expansion is linear over specific ranges of concentration corresponding to graphite's staging phenomenon [25]. Thus a linear relationship between cell strain and SOH is expected for the cells in this study, as the graphite anodes are expected to remain in stage 1 over the measured ranges of SOH.

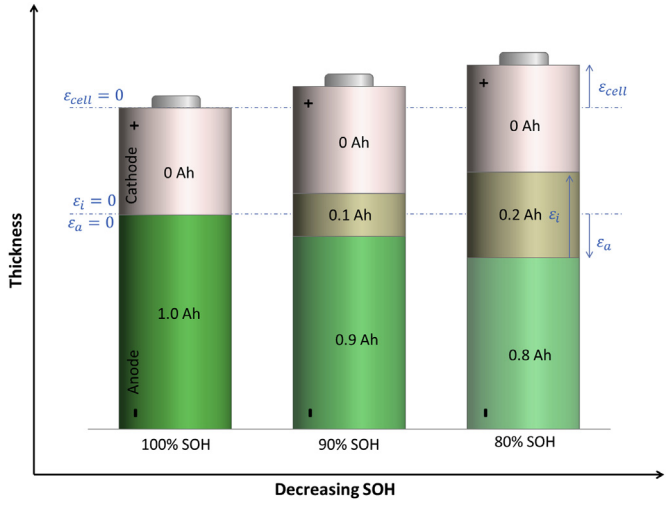

Fig. 8. Schematic showing cell expansion at 100% SOC is determined by the competing effects of decreased anode utilization and irreversible expansion. In each snapshot, the cell is fully charged such that the cathode is always in a depleted state, regardless of SOH.

Finally, we must relate the cell strain to stack stress, which is the measured quantity in this study. We first assume that increases in stack stress are due entirely to increases in cell strain, which is valid for scenarios in which no hydrostatic pressure accumulation occurs due to processes such as gas evolution, as is the case for the cells considered in this study. If we further assume that the cell exhibits linear-elastic mechanical properties such that stress σ is proportional to strain ε through a constant modulus of elasticity E, then we can express the stack stress of the charged cell as

$$\sigma = \sigma_0 + E\varepsilon_{\text{cell}} \tag{7}$$

where σ_0 is the initial stack pressure at 100% SOC and 100% SOH. Eq. (7) shows that the increase in stack stress of a charged cell is proportional to cell strain under the assumption of linear-elastic properties. The validity of this assumption is doubtful initially, as it is well known that lithium-ion cells generally exhibit non linear-elastic mechanical properties. However, the mechanical properties can be approximated as linear-elastic for small values of $\varepsilon_{\text{cell}}$. This approximation is valid when considering the stress-SOH relationship at 100% SOC, where the strain of interest is the relatively small strain arising from the competing effects of irreversible expansion (ε_i) and anode contraction (ε_a). The linear approximation breaks down when considering the relationship between stress and SOC, where the strains due to reversible electrode expansion are relatively large. The breakdown of this approximation for the stress-SOC relationship can be seen in Fig. 7, where all the curves exhibit upward concavity reminiscent of a cell stress-strain curve.

Combining Eqs. (5)–(7) gives a final expression for the stress-SOH relationship of a charged cell:

$$\sigma = \sigma_0 + E(k_i - k_a)(1 - \text{SOH}) \tag{8}$$

Eq. (8) shows that increases in stack stress are expected to be proportional to SOH under the assumptions of this analysis, which is in qualitative agreement with the experimental results presented in Figs. 1–3 and 5. An important consequence of Eq. (8) is that the stress-SOH (or strain-SOH) relationships measured for a given cell will not solely reflect the effects of irreversible expansion. Instead there will be some deviation resulting from decreased electrode utilization. For the purposes of using stress/strain for monitoring cell SOH as a practical means, this distinction between the two phenomena is unimportant. In this case, the $(k_i - k_a)$ term can be treated as a single constant, the knowledge of which is sufficient for determining SOH from stress measurements. If one were inclined to distinguish the effects of both phenomena, it would be necessary to conduct strain measurements of single electrodes [25,26] to determine the contribution of the decreased electrode utilization effect. An expression similar to Eq. (8) could be determined for a discharged cell by considering cathode contraction instead of anode contraction in the analysis. However, as a practical consideration, the stress-SOH relationship in the charged state is more useful because one would expect a battery to be regularly fully

charged during normal operation, whereas full discharge might occur irregularly and infrequently.

4. Conclusions

Mechanical measurements, of either stack stress or strain, can be used to provide real time measurements of SOH and SOC in lithium-ion cells. For the cells in this study, stack stress is linear with SOH. This simple linear relationship between stress and SOH is a distinct advantage to the complicated models used for estimating SOH. Mechanical measurements of SOC can detect self discharge and do not rely on integration, which are two advantages over conventional Coulomb counting. These results open the door for improved battery management systems through the incorporation of mechanical measurements.

The physical basis for the stress-SOH relationship is thought to be SEI growth. This is supported by the $t^{1/2}$ behavior of the stress and capacity data, as well as differential voltage spectroscopy measurements during cycling. Furthermore, stress in cells held at 4.2 V increases in the absence of cycling and increases at an accelerated rate at high temperature. If such a capacity fade mechanism is assumed, the linear stress-SOH relationship can be explained through consideration of the volume changes occurring at the electrodes and the mechanical properties of the cell. Exploitation of the relationship between expansion and degradation can be used to provide new fundamental insights in aging studies.

Acknowledgments

J.C. acknowledges the Department of Defense (DoD) for support through the National Defense Science and Engineering Graduate Fellowship (NDSEG) Program. We also acknowledge support from the Rutgers-Princeton NSF IGERT in Nanotechnology for Clean Energy.

References

[1] Y. Xing, E.W.M. Ma, K.L. Tsui, M. Pecht, Energies 4 (12) (2011) 1840–1857.
[2] L. Lu, X. Han, J. Li, J. Hua, M. Ouyang, J. Power Sources 226 (2013) 272–288.
[3] A. Barré, B. Deguilhem, S. Grolleau, M. Gérard, F. Suard, D. Riu, J. Power Sources 241 (2013) 680–689.
[4] J. Zhang, J. Lee, J. Power Sources 196 (15) (2011) 6007–6014.
[5] V. Pop, H.J. Bergveld, P.H.L. Notten, P.P.L. Regtien, Meas. Sci. Technol. 16 (12) (2005) R93–R110.
[6] H. Rahimi-eichi, Battery Management System, June 2013, pp. 4–16.
[7] V. a. Sethuraman, L.J. Hardwick, V. Srinivasan, R. Kostecki, J. Power Sources 195 (11) (2010) 3655–3660.
[8] A. Mukhopadhyay, A. Tokranov, X. Xiao, B.W. Sheldon, Electrochim. Acta 66 (0) (2012) 28–37.
[9] a. Tokranov, B.W. Sheldon, P. Lu, X. Xiao, a. Mukhopadhyay, J. Electrochem. Soc. 161 (1) (2013) A58–A65.
[10] Y.-T. Cheng, M.W. Verbrugge, J. Power Sources 190 (2) (2009) 453–460.
[11] M.J. Chon, V. a. Sethuraman, a. McCormick, V. Srinivasan, P.R. Guduru, Phys. Rev. Lett. 107 (4) (2011) 045503.
[12] J. Cannarella, C.B. Arnold, J. Power Sources 245 (2014) 745–751.
[13] T. Marks, S. Trussler, a. J. Smith, D. Xiong, J.R. Dahn, J. Electrochem. Soc. 158 (1) (2011) A51.
[14] a. J. Smith, H.M. Dahn, J.C. Burns, J.R. Dahn, J. Electrochem. Soc. 159 (6) (2012) A705.
[15] R. Deshpande, M. Verbrugge, Y.-T. Cheng, J. Wang, P. Liu, J. Electrochem. Soc. 159 (10) (2012) A1730–A1738.
[16] J. Lee, N. Nitta, J. Benson, A. Magasinski, T. Fuller, G. Yushin, Carbon 52 (2013) 388–397.
[17] I. Bloom, A.N. Jansen, D.P. Abraham, J. Knuth, S. a. Jones, V.S. Battaglia, G.L. Henriksen, J. Power Sources 139 (1–2) (2005) 295–303.
[18] E.M. Krieger, J. Cannarella, C.B. Arnold, Energy 60 (2013) 492–500.
[19] R. Fu, S.-Y. Choe, V. Agubra, J. Fergus, J. Power Sources 261 (2014) 120–135.
[20] B. Bitzer, A. Gruhle, J. Power Sources 262 (2014) 297–302.
[21] R.S. Rubino, H. Gan, E.S. Takeuchi, J. Electrochem. Soc. 148 (9) (2001) A1029.
[22] D. Liu, Y. Wang, Y. Xie, L. He, J. Chen, K. Wu, R. Xu, Y. Gao, J. Power Sources 232 (2013) 29–33.
[23] N. Zhang, H. Tang, J. Power Sources 218 (2012) 52–55.
[24] J.B. Siegel, a. G. Stefanopoulou, P. Hagans, Y. Ding, D. Gorsich, J. Electrochem. Soc. 160 (8) (2013) A1031–A1038.
[25] M. Hahn, H. Buqa, P.W. Ruch, D. Goers, M.E. Spahr, J. Ufheil, P. Novak, R. Kotz, Electrochem. Solid State Lett. 11 (9) (2008) A151.
[26] T. Ohzuku, N. Matoba, K. Sawai, J. Power Sources 98 (2001) 73–77.
[27] J. Cannarella, C.B. Arnold, J. Power Sources 226 (2013) 149–155.
[28] C. Peabody, C.B. Arnold, J. Power Sources 196 (19) (2011) 8147–8153.
[29] W. Wu, X. Xiao, X. Huang, S. Yan, Comput. Mater. Sci. 83 (2014) 127–136.
[30] I. Avdeev, M. Martinsen, A. Francis, J. Mater. Eng. Perform. (Ref. [5]).
[31] C.T. Love, J. Power Sources 196 (5) (2011) 2905–2912.
[32] R. Fu, M. Xiao, S.-Y. Choe, J. Power Sources 224 (2013) 211–224.
[33] X. Wang, Y. Sone, G. Segami, H. Naito, C. Yamada, K. Kibe, J. Electrochem. Soc. 154 (1) (2007) A14.
[34] J.H. Lee, H.M. Lee, S. Ahn, J. Power Sources 119-121 (2003) 833–837.
[35] X. Wang, Y. Sone, S. Kuwajima, J. Electrochem. Soc. 151 (2) (2004) A273.
[36] E. Sahraei, R. Hill, T. Wierzbicki, J. Power Sources 201 (2012) 307–321.
[37] S.J. Harris, P. Lu, J. Phys. Chem. C 117 (13) (2013) 6481–6492.